The electron pairing of Iron-based Superconductors

Jinchao Zhao

May 2021

Abstract

Iron-based superconductors are the second family of High-Tc superconductors people have found until now besides cuperates. This essay presents a review of experimental measurements on iron based superconductors, and aims at the difference and potential links between the pairing mechanism of these two families of high-T_c superconductors.

1 Introduction

The class of material that lose the resistance at a certain low temperature is called as superconductors, and the characteristic temperature is called the critical temperature T_c. Since its discovery in 1911, superconductivity have been regard as the most complex problem in condensed matter physics. And the research into this phenomenon has been awarded with Nobel prize for five times to eleven laureates.

The history of superconductor started with Heike Kamerlingh Onnes liquifying helium and discovering the zero resistivity in mercury below 4.2K. This exotic behavior of superconductors comes together with the other defining property, notably the Meissner effect, discovered in 1933. During the middle of 1950s, the success of the Ginzburg-Landau theory and the Bardeen-Cooper-Schrieffer(BCS) theory seems to put an undoubted end to the story according to the correctness and successful applications of them, such as the Abrikosoc cortex predicted in 1957, Giaever's tunneling experiments in 1960, and the Josephson effect predicted in 1962.

However, the period during which people think they have got everything about superconductivity ended in 1986, when Bednorz and Müller discovered $T_c = 35$K in a layered copper oxide, whose parent material is a Mott insulator. This breakthrough led to an intensive research on superconductivity in copper oxide materials which shows superconductivity with high-T_c and we call them cuprates. Within 10 years of the discovery of the cuperates, the critical temperature has risen to 138K. At the same time, extensive effort had been made to search for high-T_c superconductivity in oxides of other transition metals, though none of them has been found yet. Despite the great success on the overcoming of the critical temperature to the boiling point of liquid Nitrogen which have great applications in industry, the underlying mechanism still remains to be revealed. It was believed that the cuprates have a magnetic origin rather than phononic in BCS theory, which makes the problem complex because the behavior of low energy excitations of the spin degree of freedom, namely the spin fluctuation, is elusive[1].

It was a huge surprise when the superconductivity with $T_c = 26$K[7] was discovered in La(O, F)FeAs. In less than 2 months, T_c soared to 55K[13] in similar layered iron pnictides, just like what occurred to the cuprates, qualifying the iron-based system as the second family of high-T_c superconductors. The key difference between the iron-based superconductors(IBSC) and the cuprates is that the ground state in IBSC is metal, instead of a Mott insulator.

This essay gives an experimental review on the structure and Electromagnetic properties of the parent materials, and then introduces several kinds of the characteristic measurements including ARPES, Optical Reflection and Neutron Scattering focused on the doped superconducting phase.

2 Material Property

The discovery of IBSC started with the exploration of electro-active functionality in transparent oxides. The first doped LaFeAsO sample showed high temperature superconductivity was done by Yoichi Kamihara, a Postdoc at Hideo's group, attempted aliovalent substitution to dope the carrier, namely F-doping to the O-site[6]. We will have a experimental review mainly on the parent material LaFeAsO, also called 1111-typre iron-arsenides, as well as the characterization.

2.1 Structures of Fe-based High Tc Superconductors

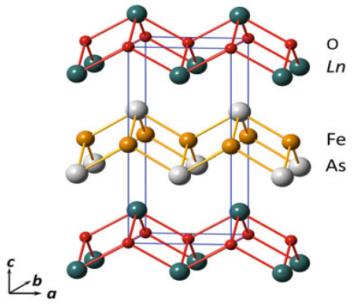

Figure 1: crystal structure of LnFeAsO

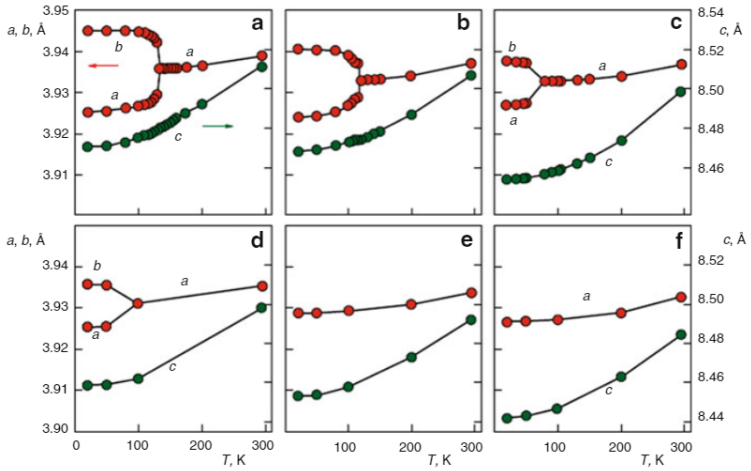

Figure 2: The temperature dependence of lattice constants for different F doping levels in $SmFeAsO_{1-x}F_x$ family. (a)$x = 0$,(b)$x = 0.05$,(c)$x = 0.10$,(d)$x = 0.12$,(e)$x = 0.15$,(f)$x = 0.20$[10]

The iron-based superconductors share the common Fe_2X_2(X = As/Se) lay-

ered structure unit, which shows an anti-PbO-type atom arrangement. Up to now, the highest T_c 56K in IBSC has been achieved in flourine-doped LnFeAsO compounds (Ln represents rare-earth metal atoms), which adopt a ZrCuSiAs-type structure and are usually briefly written as 1111 phase. LnFeAsO compounds have a tetragonal layered structure at room temperature, with space group $P4/nmm$. Figure 1 shows the schematic view of their crystal structure. The earliest discovered 1111 compound with relative high T_c is LaFeAsO.

The parent compounds of 1111 family have a remarkable feature in structure, that is, a structural transition from tetragonal to orthorhombic symmetry occurs as temperature is cooled down. The structural transition temperature(T_s) of LaFeAsO is about 155K, which is confirmed by the measurement of the temperature dependence of lattice constants in Figure 2 (a). With F-doping on the O-site, T_s decreases rapidly and the structure transition disappears as F content is larger than a critical level[10] as shown in other plot of Figure 2. In the structural transition, chemical formulae in each unit cell change from 2 to 4 with the symmetry degradation.

2.2 Electromagnetic Properties of LaT_MPnO

When a chalcogen anion (Ch) with -2 charge in LaCuOCh is replaced by a pnicogen anion (Pn) with -3, Cu^+ with $3d^{10}$ electronic configuration can be substituted by a transition metal cation (T_M) with +2. Figure 3 summarizes electromagnetic properties of LaT_MPnO hich have been clarified to date. It is obvious that the electromagnetic properties drastically vary with the number of 3d electrons in T_M.

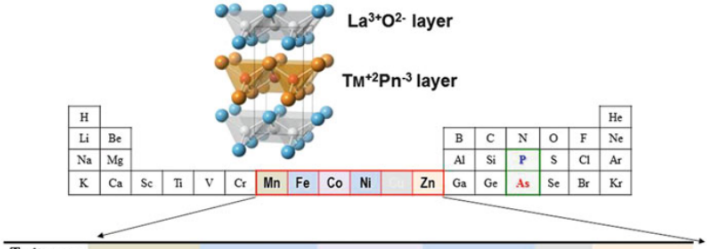

T_M^{2+}(electron configuration)	Mn($3d^5$)		Fe($3d^6$)		Co($3d^7$)		Ni($3d^8$)		(Cu)	Zn($3d^{10}$)	
Pn	P	As	P	As	P	As	P	As		P	As
Elect. Prop.	Mott Insulator		Superconductor		Metal		Superconductor		–	Semiconductor	
Magnetism	AF				FM				–	Non-magnetic	
E_g	~1 eV		–		–		–		–	~1.5 eV	
T_C (SC) T_{NC}(Mag.)	> 400 K		Undoped: 4 K	F-doped: 26 K	43 K	66 K	Undoped: 3 K	Undoped: 2.4 K		–	
Ref.	Yanagi et al JAP (2009)		Kamihara et al. JACS(2006), Kamihara et al. JACS (2008)		Yanagi et al. PRB (2008)		Watanabe et al. IC (2007), Watanabe et al. JSSC (2007)		–	Kayanuma et al. PRB (2007), Kayanuma et al. TSF (2008)	

Figure 3: Summary of electromagnetic properties of LaT_MPnO. T_M: 3d transition metal, and Pn = P/As)

It is noted that the system of T_M with odd number of 3d electrons has long range spin ordering and does not exhibit superconductivity, whereas the system of T_M with even 3d electron number is a Pauli paramagnetic metal and exhibits superconductivity. Among them is the LaFeAsO with T_M = Fe. It is a Pauli paramagnetic metal at high temperatures but as T decreases, a sudden decrease in resistivity and magnetic susceptibility occurs at 160K, reaches a minimum, and increases as in Figure 4 (b). F-doping to the O-site induced a drastic change in the ρ–T curves. As the F-content increases, zero-resistivity began to appear at $T > 4$ K above $F > 4$ mol% and this temperature went up to 32 K(onset) at F=11 %. We noted the emergence of Tc accompanies the disappearance of sudden ρ-drop around 160 K.

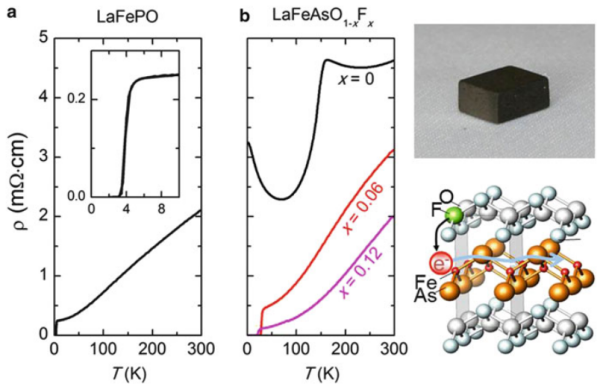

Figure 4: Temperature dependence of resistivity in polycrystalline LaFePO and $LaFeAsO_{1-x}F_x$[7]. The upper right shows the photo of $LaFeAsO_{0.88}F_{0.12}$

In the present IBSCs, electron-doping induces superconductivity by suppressing the crystallographic transition of high-symmetrical tetragonal phase to a low-symmetry phase which stabilizes the AF spin ordering. Though surprisingly, a coexistant state of the SDW ordering and superconductivity was widely observed in 122-type IBSC materials since magnetic orders are supposed to scatter the cooper pair and thus make the superconducting state unstable. For the doped 122 materials, the question of whether the SDW and superconducting states are microscopically coexisting or phase separated has received considerable attentions experimentally. In the isovalent doped "122" materials, the microscopic coexistence of superconductivity and SDW ordering was confirmed by NMR experiments[9].

2.3 Phase Diagram

In order to achieve superconductivity, chemical doping or applying external/ chemical pressure on parent compounds of iron-based superconductors is always necessary. By various chemical doping or external pressure, the ground states

of iron-based superconductors could be well-tuned from antiferromagnetic to superconducting phases, and exhibit a quite universal phase diagram similar to those of cuprate superconductors. This suggests a possible universal mechanism in both high-T_c superconductor families.

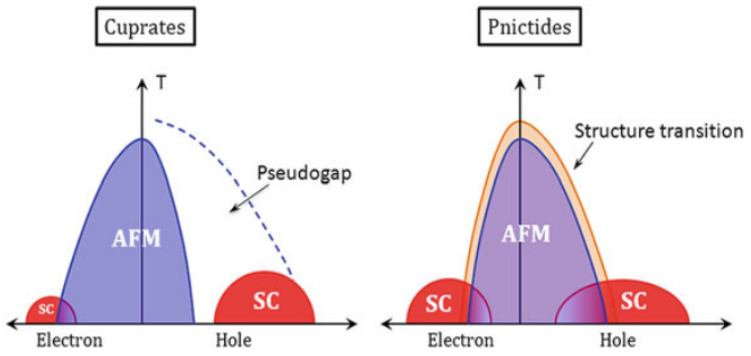

Figure 5: The universal electronic phase diagram in cuprate and pnictide superconductors

In the general phase diagram as shown in Figure 5, the parent compounds of iron-based superconductors exhibit antiferromagnetic ordering at low temperature. Considering that it behaves as a poor metal, the mechanism of such antiferromagnetism was historically ascribed to spin-density-wave (SDW) ordering of itinerant electrons at beginning[3]. In contrast, the mechanism of antiferromagnetism in cuprates was ascribed to superexchange of local moments. With decreasing temperature, the parent compounds also exhibit an interesting structural transition from high-temperature tetragonal structure to low-temperature orthorhombic structure[10]. T_s is usually slightly higher than or even equal to the antiferromagnetic transition temperature (T_N). Such structural transition is ascribed to electron-driven phase transition rather than pure structural effect, and strongly couple to the following antiferromagnetic transition.

By choosing different chemical doping, we could dope hole- or electron-type carriers into parent compound and achieve superconductivity in both cases in certain doping range. As shown in Figure 5, both of structural and antiferromagnetic transitions are suppressed continuously by doping both carriers. Meanwhile, superconductivity starts to emerge above critical doping level and coexists with suppressed SDW order in part of the phase diagram, and finally reaches a maximum optimal doping level. The whole superconducting region shows a dome-like shape in the phase diagram.

As discussed in the previous section, the coexistence of SDW and superconducting states draw great interests. The intersection part of the phase diagram will be further discussed in the section about neutron scattering experiments.

3 Characterization of the Superconductivity

3.1 Electron Spectroscopy: ARPES

Angle-resolved photoemission spectroscopy (ARPES) is a powerful technique that can directly probe the electronic structure of materials in the momentum space. With ultra-high energy and momentum resolutions, ARPES can help to understand how materials behave. Especially, for high-Tc superconductors, the experimental results from ARPES, including the Fermi surface, band dispersion, energy kink, superconducting gap distribution, etc., serve as solid foundations for our understanding on the superconductivity.

3.1.1 The Undoped Compounds

According to the BCS theory, the cooper pair are coupled between the electrons in adjacent to the fermi surface. Thus it's very important to understand the Fermi surface topology for constructing the theoretical models. For iron-based superconductors, unlike the cuprates where the superconductivity is induced by doping a Mott insulator, the parent compounds of IBSCs are metals. Early band calculations all showed that the low-lying electronic structure is dominated by the Fe $3d^6$ electrons. The Fermi surface is consisted of three hole pockets at the zone center($\alpha, \beta, \text{and}\gamma$), and two electron pockets at the zone corner ($\delta, \text{and}\eta$). See Figure 6

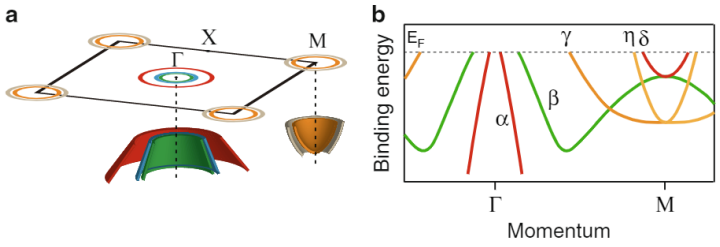

Figure 6: (a) The illustration of the general Fermi surface topology. (b) The $\Gamma - M$ band dispersion for iron-based superconductors.

3.1.2 The Effect of Carrier Doping

Similar to the cuprates, the superconductivity in IBSCs could be induced by doping carriers. We took two systems as examples, the hole doped $Ba_{1-x}K_xFe_2As_2$ and the electron doped $NaFe_{1-x}Co_xAs$[14]. In Figure 7 with hole doping, the center hole pockets expand, while the corner electron pockets shrink. A Lifshitz transition(change of Fermi surface topology) occurs when the electron pockets disappear at the zone corner and four propeller-like hole pockets develop. Things reverse for the electron doped side, where the center hole pockets shrink and the corner electron pockets expand with the increase of electron doping. Early the-

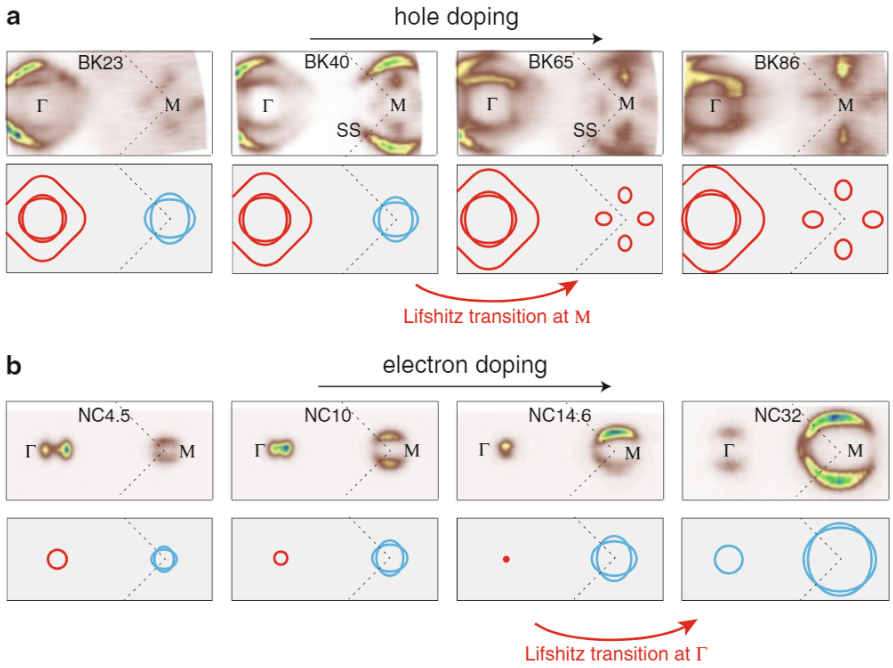

Figure 7: The doping dependence of Fermi surface topology in: (a) hole doped $Ba_{1-x}K_xFe_2As_2$; (b) electron doped $NaFe_{1-x}Co_xAs$[14]

oretical studies all pointed out that the superconducting pairing in iron-based superconductors is mediated by the inter-pocket scattering between the central hole and the corner electron pockets[8]. In this scenario, Tc only could be optimized when both central hole and corner electron pockets are present. However, the discovery of high-Tc superconductivity in heavily electron doped iron-chalcogenide[12] strongly challenges this inter-pocket superconducting pairing in iron-based superconductors. These heavily electron doped Iron-chalcogenides only have electron pockets in the Brillouin zone without any center hole pockets. They are called the second class iron-based superconductors, and whether the topology change in Fermi surface play a role in determining Tc still remains to be revealed.

3.1.3 The Superconducting Gap and Pairing Symmetry

The pairing symmetry of Cooper pair is a pivotal characteristic for a superconductor. ARPES can directly map out the superconducting gap distribution in the momentum space, which gives strong constraints on determining the pairing symmetry of superconductors. For IBSCs, three kinds of pairing symmetry were mostly proposed. They are all s-wave like, but with different phases on each

Fermi surface sheets as shown in Figure 8. There is no sign change in S_{++} pairing symmetry. For $S_{\pm}$ pairing symmetry, the phases change sign between the center hole pockets and the corner electron pockets. For S_{odd} pairing symmetry, the sign change occurs within the center hole and corner electron pockets.

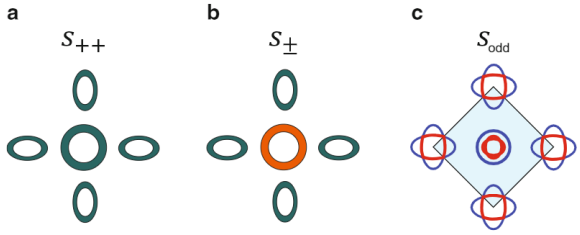

Figure 8: The illustration of the gap symmetries predicted in iron-based superconductors

The ARPES measurement on superconducting gap was first done in optimal doped $Ba_{1-x}K_xFe_2As_2$[2]. The gap distribution in k_x–k_y plane is illustrated in Figure 9. It is nodeless and isotropic on all the Fermi surface sheets and this universality was also observed in various compounds. The nodeless andisotropic superconducting gap observed here is consistent with all three pairing symmetries proposed by theories.

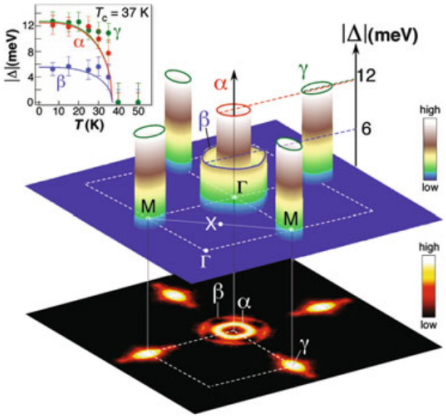

Figure 9: The superconducting gap distribution measured in $Ba_{1-x}K_xFe_2As_2$[2]

3.2 Optical and Transport Properties

The optical properties of a material yield a tremendous amount of information about the transport and electronic properties. Particularly, the optical

signatures of the opening of a superconducting gap are the increase in the low-frequency reflectance and the rapid decrease in the low-frequency conductivity, or spectral weight, in response to the formation of a superconducting condensate. This may result the transfer of low-frequency spectral weight into a zero-frequency delta function.

3.2.1 Resistivity

The resistivity of single crystals of LaFeAsO reveals a highly anisotropic response with a resistivity ratio of $\rho_{ab}/\rho_c \approx 20 - 200$, which is consistent with the layered structure of these materials. Within the family of materials REFeAsO (RE=La,Nd and Sm),there is also a resistivity anomaly that is associated with a structural and magnetic transition, showed in Figure 10, below which the resistivity continues to decrease.

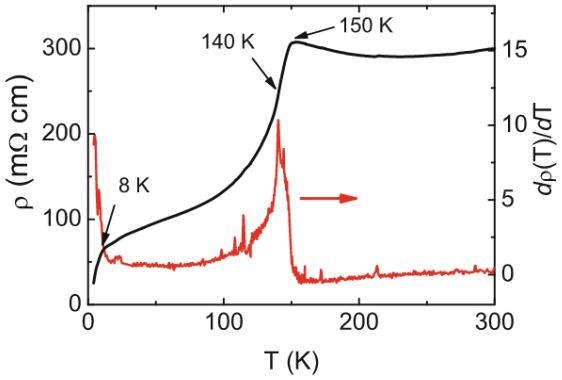

Figure 10: The temperature dependence of the in-plane resistivity for NdFeAsO[4]

3.2.2 Optical Conductivity

The detailed temperature dependence of the in-plane reflectance of NdFeAsO is shown in Figure 11. The Drude-like component narrows with decreasing temperature until ≈150K, below which there is a dramatic redistribution of spectral weight from low to high frequency with decreasing temperature; while the Drude-like component loses weight, it also narrows dramatically.

3.3 Neutron Scattering

Over the past several years, much progress has been made in characterizing the magnetism in cuprates. It is well known that the parent compounds of copper oxide superconductors are Mott insulators . Superconductivity can be induced by charge carrier doping within the Cu–O plane or away from it, resulting

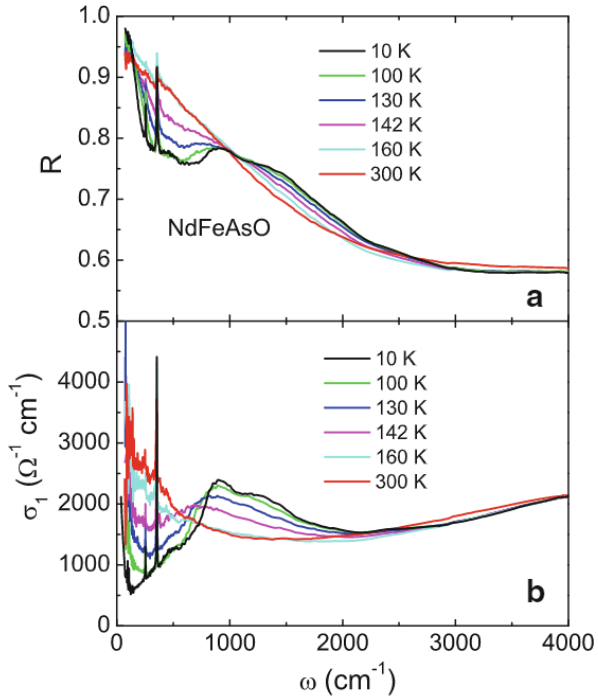

Figure 11: The temperature dependence of (a) the reflectance and (b) the real part of the optical conductivity of NdFeAsO[4]

many competing phases to superconductivity. Compared with copper oxide superconductors, a systematic investigation of spin dynamics in iron pnictide superconductors has some unique advantages including the growth of large sized single crystal of IBSCs.

3.3.1 Antiferromagnetic Order

Neutron diffraction measurements have established the long range AF order in these parent compounds. Results are showed in Figure 12. The spins of Fe^{2+} are AF along the a-direction and ferromagnetic along the b-direction while the spins of Cu^{2+} are aligned anti-parallel in both directions.

3.3.2 Phase Diagram

Upon doping electrons or holes into the parent compounds, the long range AF order is gradually suppressed with reduced T_N and ordered moment. In copper oxide superconductors, static incommensurate AF order can arise from spin and charge separation (stripes) or a spin glass state. In the neutron scattering work on $Ba(Fe_{1-x}Co_x)_2As_2$,it is suggested that the separated Ts and T_N smoothly

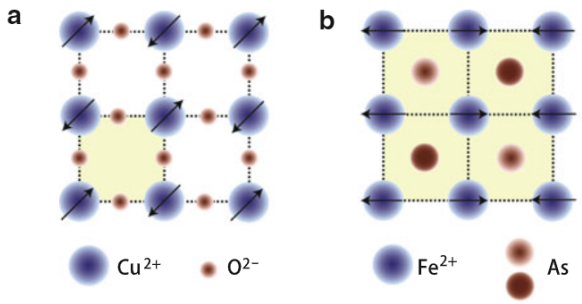

Figure 12: Magnetic structures for (a) the parent material for cuperate High-Tc superconductors La_2CuO_4;(b) the parent material for 1111, 111 and 112 type IBSCs

extend into the super-conducting dome and bend back below Tc[11], resulting in distinct structuraland magnetic quantum critical points (QCPs) at different x, see Figure 13

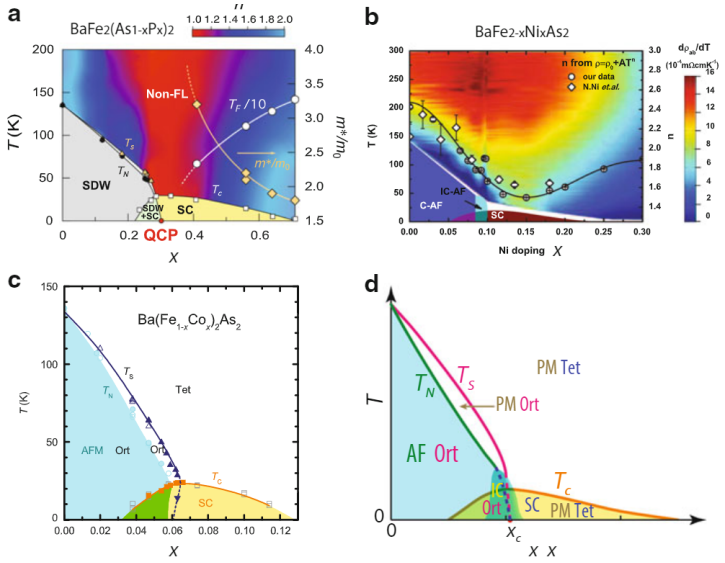

Figure 13: Electronic phase diagrams of some IBSC, name are labeled in figures

4 Conclusion

As the second family of High-Tc Superconductors, Iron-based superconductors possesses a lot of common properties such as 3d electron induced AF ordering

in parent materials and symmetry behavior in electron and hole doping region. The pairing mechanism, however, is a much more complicated problem in IBSCs because of the multi-band nature of the system, as well as the symmetry breaking phase transform in the parent materials.

In recent experiments, there have been reported that with further electron doping using H^- instead of F^- doping, a 2-dome superconducting region was discovered in 1111-system, showed in Figure 14[5]. The appearance of the Tc double structure and different nature for each dome implied the presence of different parent phases. An AFM structure withNeel temperature and tetra-ortho crystallographic phase transition temperature of ≈75 K was found for x=0.5. These findings suggest the intimate interplay between the magnetic interaction, structural changes, and orbital degree of freedom in this system. The discovery of bipartite magnetic parentphases provides a view that higher Tc in LnFeAsO is a consequence of an optimizedcondition of two factors with different nature such as a spin and an orbital.

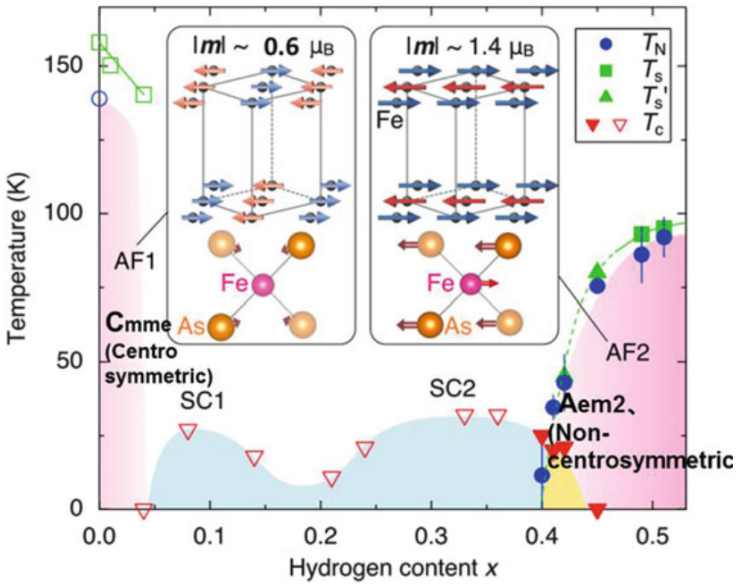

Figure 14: Phase diagram of $LaFeAsO_{1-x}H_x$. Note that there exit two AFM-phases with different properties

References

[1] Gorachand Biswal and KL Mohanta. A recent review on iron-based superconductor. *Materials Today: Proceedings*, 35:207–215, 2021.

[2] Hong Ding, P Richard, Kosuke Nakayama, Katsuaki Sugawara, Toshiyuki Arakane, Y Sekiba, Akari Takayama, Seigo Souma, Takafumi Sato, Takashi Takahashi, et al. Observation of fermi-surface–dependent nodeless superconducting gaps in ba0. 6k0. 4fe2as2. *EPL (Europhysics Letters)*, 83(4):47001, 2008.

[3] Jing Dong, HJ Zhang, Guizhou Xu, Zhengcai Li, Gang Li, WZ Hu, Dan Wu, GF Chen, Xi Dai, JL Luo, et al. Competing orders and spin-density-wave instability in la (o1- xfx) feas. *EPL (Europhysics Letters)*, 83(2):27006, 2008.

[4] T Dong, ZG Chen, RH Yuan, BF Hu, B Cheng, and NL Wang. Formation of partial energy gap below the structural phase transition and the rare-earth element-substitution effect on infrared phonons in r e feaso (r e= la, nd, and sm). *Physical Review B*, 82(5):054522, 2010.

[5] Soshi Iimura, Satoru Matsuishi, Hikaru Sato, Taku Hanna, Yoshinori Muraba, Sung Wng Kim, Jung Eun Kim, Masaki Takata, and Hideo Hosono. Two-dome structure in electron-doped iron arsenide superconductors. *Nature communications*, 3(1):1–7, 2012.

[6] Peter D Johnson, Guangyong Xu, and Wei-Guo Yin. *Iron-based superconductivity*, volume 211. Springer, 2015.

[7] Yoichi Kamihara, Takumi Watanabe, Masahiro Hirano, and Hideo Hosono. Iron-based layered superconductor la [o1-x f x] feas (x= 0.05- 0.12) with t c= 26 k. *Journal of the American Chemical Society*, 130(11):3296–3297, 2008.

[8] Kazuhiko Kuroki, Seiichiro Onari, Ryotaro Arita, Hidetomo Usui, Yukio Tanaka, Hiroshi Kontani, and Hideo Aoki. Unconventional pairing originating from the disconnected fermi surfaces of superconducting lafeaso 1-x f x. *Physical Review Letters*, 101(8):087004, 2008.

[9] Y Laplace, J Bobroff, F Rullier-Albenque, D Colson, and A Forget. Atomic coexistence of superconductivity and incommensurate magnetic order in the pnictide ba (fe 1- x co x) 2 as 2. *Physical Review B*, 80(14):140501, 2009.

[10] Serena Margadonna, Yasuhiro Takabayashi, Martin T McDonald, Michela Brunelli, G Wu, RH Liu, XH Chen, and Kosmas Prassides. Crystal structure and phase transitions across the metal-superconductor boundary in the smfeaso 1- x f x (0 x 0.20) family. *Physical Review B*, 79(1):014503, 2009.

[11] S Nandi, MG Kim, Andreas Kreyssig, RM Fernandes, DK Pratt, A Thaler, Ni Ni, Sergey L Bud'ko, Paul C Canfield, J Schmalian, et al. Anomalous suppression of the orthorhombic lattice distortion in superconducting ba (fe 1- x co x) 2 as 2 single crystals. *Physical Review Letters*, 104(5):057006, 2010.

[12] Wang Qing-Yan, Li Zhi, Zhang Wen-Hao, Zhang Zuo-Cheng, Zhang Jin-Song, Li Wei, Ding Hao, Ou Yun-Bo, Deng Peng, Chang Kai, et al. Interface-induced high-temperature superconductivity in single unit-cell fese films on srtio3. *Chinese Physics Letters*, 29(3):037402, 2012.

[13] Zhi-An Ren, Jie Yang, Wei Lu, Wei Yi, Guang-Can Che, Xiao-Li Dong, Li-Ling Sun, and Zhong-Xian Zhao. Superconductivity at 52 k in iron based f doped layered quaternary compound pr [o1–xfx] feas. *Materials Research Innovations*, 12(3):105–106, 2008.

[14] LX Yang, Y Zhang, HW Ou, JF Zhao, DW Shen, B Zhou, J Wei, F Chen, M Xu, C He, et al. Electronic structure and unusual exchange splitting in the spin-density-wave state of the bafe 2 as 2 parent compound of iron-based superconductors. *Physical review letters*, 102(10):107002, 2009.